Molecular Biology of the Cell
Vol. 16, 1744–1755, April 2005

Rab11 in Recycling Endosomes Regulates the Sorting and Basolateral Transport of E-Cadherin[V]

John G. Lock* and Jennifer L. Stow*†

*Institute for Molecular Bioscience and the †School of Molecular and Microbial Sciences, The University of Queensland, Brisbane, 4072 Australia

Submitted October 5, 2004; Revised January 13, 2005; Accepted January 19, 2005
Monitoring Editor: Jennifer Lippincott-Schwartz

E-cadherin plays an essential role in cell polarity and cell-cell adhesion; however, the pathway for delivery of E-cadherin to the basolateral membrane of epithelial cells has not been fully characterized. We first traced the post-Golgi, exocytic transport of GFP-tagged E-cadherin (Ecad-GFP) in unpolarized cells. In live cells, Ecad-GFP was found to exit the Golgi complex in pleiomorphic tubulovesicular carriers, which, instead of moving directly to the cell surface, most frequently fused with an intermediate compartment, subsequently identified as a Rab11-positive recycling endosome. In MDCK cells, basolateral targeting of E-cadherin relies on a dileucine motif. Both E-cadherin and a targeting mutant, ΔS1-E-cadherin, colocalized with Rab11 and fused with the recycling endosome before diverging to basolateral or apical membranes, respectively. In polarized and unpolarized cells, coexpression of Rab11 mutants disrupted the cell surface delivery of E-cadherin and caused its mistargeting to the apical membrane, whereas apical ΔS1-E-cadherin was unaffected. We thus demonstrate a novel pathway for Rab11 dependent, dileucine-mediated, μ1B-independent sorting and basolateral trafficking, exemplified by E-cadherin. The recycling endosome is identified as an intermediate compartment for the post-Golgi trafficking and exocytosis of E-cadherin, with a potentially important role in establishing and maintaining cadherin-based adhesion.

INTRODUCTION

E-cadherin is a key cell-cell adhesion protein in epithelial cells. It is concentrated in adherens junctions at the lateral cell surface, where it mediates calcium-dependent, homotypic binding to cadherins on adjacent cells (Takeichi, 1991, 1995). E-cadherin function is required for morphogenesis, the maintenance of epithelial function, and as a tumor suppressor (Gumbiner, 1996; Hazan *et al.*, 2004). The cytoplasmic tail of E-cadherin supports interactions with catenins, including β-catenin and p120ctn, and through them interacts with the actin cytoskeleton and signaling proteins (reviewed by Yap *et al.*, 1997). In recent years it has become evident that E-cadherin is actively and dynamically trafficked to and from the cell surface. Both exocytic and endocytic transport contribute to the modulation of E-cadherin levels within adherens junctions, thereby providing one mechanism for regulating adhesion (reviewed in Bryant and Stow, 2004). In polarized epithelia, a small proportion of surface E-cadherin is endocytosed and recycled, potentially allowing for dynamic regulation of adhesion (Le *et al.*, 1999). The cytoplasmic tail of E-cadherin contains a dileucine sorting motif that is crucial for the accurate basolateral targeting of newly synthesized E-cadherin (Miranda *et al.*, 2001). Removal of this dileucine motif results in the aberrant apical delivery of a ΔS1-E-cadherin mutant protein (Miranda *et al.*, 2001, 2003), implicating an as yet unidentified adaptor complex in this basolateral transport. Other events during the basolateral trafficking of E-cadherin include sequential binding of the catenins. β-catenin associates with E-cadherin early after biosynthesis (Chen *et al.*, 1999), whereas our recent studies show that in MDCK cells, p120ctn binds to E-cadherin at or near the basolateral surface (Miranda *et al.*, 2003). Interestingly, p120ctn has recently been shown to bind directly to a microtubule motor protein of the kinesin family, forming an indirect link between kinesin and N-cadherin, thus facilitating N-cadherin surface delivery within pleiomorphic vesicles (Chen *et al.*, 2003).

The precise route taken by E-cadherin from the *trans*-Golgi network (TGN) to the cell surface in either polarized or nonpolarized cells, is not known. Furthermore, specific regulators of this process are yet to be identified. Recent studies have identified a number of molecules involved more generally in the regulation of basolateral protein transport. Among these are the exocyst complex, and the small GTPases Rab8 and Cdc42, each of which has been demonstrated to regulate basolateral trafficking of vesicular stomatitis virus glycoprotein (VSVG; Kroschewski *et al.*, 1999; Cohen *et al.*, 2001). The exocyst, also referred to as the Sec6/8 complex, is localized in a zone of high exocytic activity, adjacent to the apical junctional complex in the lateral membrane of polarized MDCK cells (Grindstaff *et al.*, 1998; Lipschutz *et al.*, 2000; Kreitzer *et al.*, 2003). Expression-based or functional disruption of any of the eight exocyst subunits

This article was published online ahead of print in *MBC in Press* (http://www.molbiolcell.org/cgi/doi/10.1091/mbc.E04–10–0867) on February 2, 2005.

[V] The online version of this article contains supplemental material at *MBC Online* (http://www.molbiolcell.org).

Address correspondence to: Jennifer L. Stow (j.stow@imb.uq.edu.au).

Abbreviations used: AP, adaptor protein (complex); ctn, catenin; mRFP, monomeric red fluorescent protein; GGA, Golgi-localized, gamma ear-containing, ADP ribosylation factor-binding protein; LDLR, low-density lipoprotein receptor; MDCK, Madin-Darby canine kidney; PGC, post-Golgi carrier; PM, plasma membrane; SNARE, soluble *N*-ethyl maleimide–sensitive factor [NSF] attachment protein [SNAP] receptor; TGN, *trans*-Golgi network; VSVG, vesicular stomatitis virus glycoprotein.

has been demonstrated to block or cause missorting of proteins specifically associated with the basolateral transport pathway (Grindstaff *et al.*, 1998; Yeaman *et al.*, 2001; Moskalenko *et al.*, 2002; Inoue *et al.*, 2003). Rab8 and Cdc42 are thought to regulate the transport of a specific subpopulation of basolaterally targeted proteins, namely, those dependent on interaction with the μ1B adaptor subunit of adaptor protein complex 1 (AP-1; Kroschewski *et al.*, 1999; Musch *et al.*, 2001; Ang *et al.*, 2003). Rab8 is associated with recycling endosomes, and expression of a constitutively active mutant of Rab8 led to the mistargeting of a number of μ1B-dependent, basolaterally targeted protein cargoes, including VSVG and the low-density lipoprotein receptor (LDLR).

The GTPase Rab11 is distributed across a variety of intracellular post-Golgi membranes, including the TGN, recycling endosomes, the apical recycling endosome of polarized cells and specialized membrane compartments within regulated secretory cells (Calhoun and Goldenring, 1996; Goldenring *et al.*, 1996; Sheehan *et al.*, 1996; Ullrich *et al.*, 1996; Ren *et al.*, 1998). Having been first localized to the TGN and TGN-derived membranes (Urbe *et al.*, 1993), Rab11 has since been implicated in regulating the post-Golgi trafficking of VSVG in nonpolarized cells, with dominant negative Rab11 mutants causing inhibition of VSVG surface delivery (Chen *et al.*, 1998). Rab11 has also been shown to associate with actin filament bundles, along with the basolateral membrane SNARE protein, Syntaxin 4 (Band *et al.*, 2002). In this study we have used imaging of live and fixed cells to track the post-Golgi exocytosis of E-cadherin. E-cadherin leaving the TGN is delivered to an intermediate compartment, identified as a Rab11-positive recycling endosome. We show that Rab11 has key roles in the trafficking and basolateral targeting of E-cadherin.

MATERIALS AND METHODS

Cell Culture and Transfection

MDCK cells were grown as confluent monolayers in DMEM containing 2% L-glutamine and 10% fetal calf serum (FCS), as described previously (Miranda *et al.*, 2001). HeLa cells were grown to a subconfluent state in DMEM containing 2% L-glutamine and 10% FCS. Cells were transfected using Lipofectamine 2000 reagent (Life Technologies, Carlsbad, CA) combined with 2 μg of DNA per well of a six-well culture dish, according to the manufacturer's instructions. Transfected cells were used for experiments within 3–48 h. Plasmids encoding full-length human E-cadherin (hEcad), ΔS1-E-cadherin (ΔS1-Ecad), E-cadherin-GFP (Ecad-GFP), and ΔS1-E-cadherin-GFP (ΔS1-Ecad-GFP), have been previously described in Miranda *et al.* (2001, 2003). pcDNA-Ecad-YFP contains the YFP coding sequence fused in-frame to the C terminus of the human E-cadherin cytoplasmic domain and was prepared using the same protocol reported for pcDNA-Ecad-GFP (Miranda *et al.*, 2003). Primers used for the amplification of mRFP contained *Sac*II and *Xba*I restriction sites. GFP was excised from the pcDNA Ecad-GFP vector, with *Sac*II and *Xba*I endonucleases, and replaced by the mRFP coding sequence. A plasmid encoding VSVG-GFP was kindly provided by Jennifer Lippincott-Schwartz (National Institutes of Health, Bethesda, MD). CDNAs encoding the full-length sequence of Rab11a tagged with GFP (Rab11wt-GFP), constitutively active Rab11Q70L-GFP (Rab11QL-GFP; Ullrich *et al.*, 1996), and dominant negative Rab11S25N-GFP (Rab11SN-GFP) mutants of Rab11a, were kindly provided by Robert Parton (University of Queensland). The plasmid encoding Rab5 Q79L GFP (Rab5QL-GFP) has been described previously (Bryant *et al.*, 2005).

Antibodies

A mouse monoclonal antibody (mAb; Transduction Laboratories, Lexington, KY) raised against GM130 was used as a marker of the Golgi complex. HECD1, a mouse mAb (from Dr M. Takeichi, Kyoto University), was used to detect human E-cadherin. The secondary antibody used was Cy3-conjugated sheep anti-mouse IgG (Jackson ImmunoResearch Laboratories, West Grove, PA). Tetramethyl rhodamine–conjugated phalloidin was used to label F-actin (Molecular Probes, Eugene, OR), and DAPI was used to label nuclei (Molecular Probes).

Indirect Immunofluorescence

Cells grown on glass coverslips were fixed in 4% paraformaldehyde for 90 min, then washed, and permeabilized using 0.1% Triton X-100 for 5 min. Cell washes and incubations were carried out in phosphate-buffered saline (PBS) containing 0.5% bovine serum albumin. Cells were incubated first with primary antibodies for 1–2 h, followed by washing and incubation with fluorescently conjugated secondary antibodies for 1 h and final washing. For double-labeling, cells were then washed in PBS/bovine serum albumin, and fixed in 4% PFA for a further 5 min, before a second round of primary and secondary antibody labeling. The coverslips were mounted in 50% glycerol containing DABCO (1,4-diazabiccyclo-2,2,2-octane; Sigma Chemical Co., St. Louis, MO) and viewed using either epifluorescence or confocal fluorescence microscopy. Epifluorescence microscopy was performed using an Olympus IX71 inverted microscope (Olympus Australia, Mt. Waverley, Australia) and equipped with a 60× oil objective and an IMAGO Super VGA 12-bit 1280 × 1024 pixel CCD camera (TILL Photonics, Martinsried, Germany). Multicolor images were assembled using Adobe Photoshop (San Jose, CA). Confocal microscopy was performed using an LSM 510 META (Carl Zeiss Microscope Systems, Jena, Germany), utilizing optical spectral separation or digital emission fingerprinting, where appropriate. XZ and 3D reconstructions were generated using LSM 510 META software (Cambridge, MA).

Live Cell Imaging

Videomicroscopy was performed on individual live cells in sparse cultures grown on 25-mm round coverslips. During imaging, cells were immersed in CO^2-independent medium (Life Technologies, Grand Island, NY), warmed to 37°C using a heated microscope stage mount. Cell temperature is maintained to within ±0.2°C of target temperature using a heated water bath (Axyos, Brisbane, Australia) pumping water through a stage-mounted heating block. Fluorophores are excited using the Polychrome IV Xenon lamp-based monochromatic light generator, controlled by a DSP board (TILL Photonics), and viewed using an Olympus IX71 inverted microscope equipped with an Olympus 60× oil objective. Images were captured by an IMAGO Super VGA 12 bit 1280 × 1024 pixel CCD camera (TILL Photonics). Maximal imaging rates exceed 10 images per second depending on sample fluorescent intensity. Imaging control and postcapture image analysis are performed using TILLvisION software. Delays between image capture range from 0.1 s to 10 min. Total movie capture periods range from 30 s to 3 h. Movie playback speeds range from 4 to 12 frames per second. Movies are cropped, constructed, and analyzed using Image J v1.31 or TILLvisION software and associated Macro programs.

RESULTS

Exocytic Trafficking of Ecad-GFP in HeLa Cells

The post-Golgi trafficking of Ecad-GFP was initially examined in HeLa cells which, because of their flattened morphology, are optimal for these studies utilizing high-resolution live epifluorescence imaging. Ecad-GFP–transfected HeLa cells at 80% confluence were fixed and imaged, 24 h after transfection. HeLa cells do not express endogenous E-cadherin, but overexpressed, newly synthesized Ecad-GFP was found in the perinuclear Golgi complex, where it colocalized with GM130, and thereafter at the plasma membrane (PM) in newly forming adhesion junctions (Figure 1, A–E). The maximal concentration of newly synthesized Ecad-GFP fluorescence was observed in the perinuclear Golgi region at 3 h after transfection (Figure 1). This condition was used hereafter for live imaging studies focusing on the exit of Ecad-GFP from the Golgi complex and its transport to the PM.

Ecad-GFP Is Transported in Pleiomorphic Tubulovesicular Carriers

Preliminary epifluorescence imaging of live HeLa cells revealed that Ecad-GFP exits the Golgi region in pleiomorphic tubulovesicular carriers, ranging along a size continuum from spherical carriers (250 nm diameter), to tubules 1–20 μm in length (Figure 1, F–J). These post-Golgi carriers (PGCs) were compared in cells expressing either Ecad-GFP or VSVG-GFP as cargo. Overall, the characteristics, both visual and kinetic, displayed by Ecad-GFP-positive PGCs (Figure 1, F–J), were similar in all respects to PGCs containing VSVG-GFP (Figure 1, K and L). Furthermore, our obser-

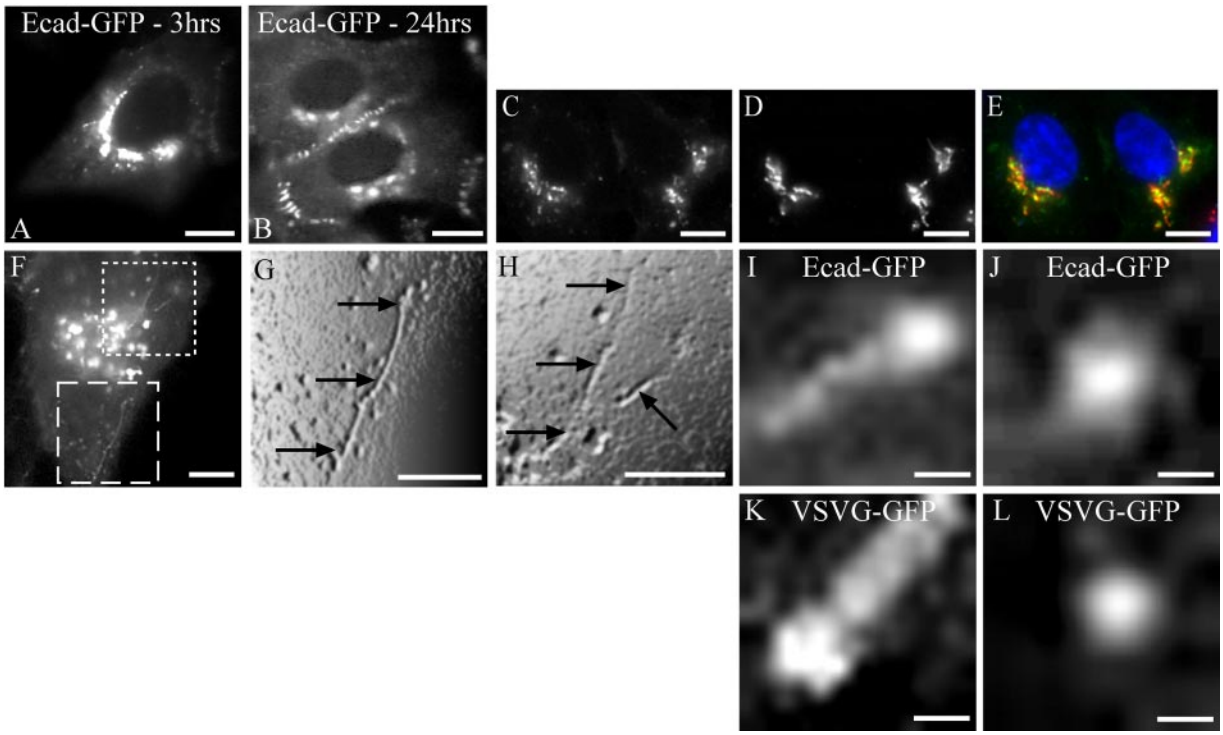

Figure 1. Expression of Ecad-GFP and transport in PGCs. HeLa cells were transiently transfected with Ecad-GFP (A–J) or VSVG-GFP (K and L). Ecad-GFP is concentrated in the perinuclear region 3 h after transfection (A) and is then visible at the PM in cell-cell contacts by 24 h (B). Shortly after transfection, newly synthesized Ecad-GFP (C) and the Golgi marker GM130 (D) colocalize in a merged image (E) in fixed HeLa cells. Ecad-GFP is visible in the Golgi region and in PGCs exiting the Golgi in a live HeLa cell (F). Regions from the image in F are magnified, digitally filtered and shown in relief to demonstrate two regions of interest containing Ecad-GFP–positive tubular PGCs (dashed box shown in G; dotted box shown in H). Arrows show tubular PGCs (5–20 μm; G and H), as they exit the Golgi region. Individual PGCs imaged after exit from the Golgi carrying either Ecad-GFP (I and J) or VSVG-GFP (K and L), from different transfected cells, include tubulovesicular PGCs ($\sim$1 μm length) with concentrations of cargo at the trailing edge (I and K) or spherical carriers (250–300 nm diameter; J and L). Scale bars, (A–H) 10 μm; (I–L) 200 nm.

vations correlate closely with previously published analyses of the characteristics of post-Golgi transport carriers (Hirschberg *et al.*, 1998; Toomre *et al.*, 1999; Polishchuk *et al.*, 2000, 2003). Thus, Ecad-GFP is transported in carriers of a type indistinguishable from those commonly demonstrated for VSVG-GFP transport.

Ecad-GFP Carriers Utilize Two Alternative post-Golgi Routes

The movement and trajectories of PGCs were analyzed after live image sequence capture. PGCs exhibited largely unidirectional curvilinear motion as they exited the Golgi region, with the majority moving radially away from the Golgi complex, consistent with the movement and microtubule-based transport of post-Golgi tubulovesicular carriers reported by others (Toomre *et al.*, 1999). Some PGCs were also tracked heading centripetally, toward the perinuclear region in the *XY* plane, indicating some variety in the directional movement of carriers. The maximal rate of movement observed for PGCs was $\sim$3 μm/s and was not dependent on carrier size. Tubular PGCs displayed the ability to bifurcate, subdivide, fuse, and to extend and retract during budding from the Golgi complex. PGC paths were imaged and then identified and delineated using sequential back-subtraction, resulting in the observation that Ecad-GFP-positive PGCs are largely excluded from the lateral periphery of the cell, with most post-Golgi trafficking routes concentrated in a midcellular region (Figure 2).

The fates and post-Golgi trafficking routes of Ecad-GFP PGCs were analyzed at high-resolution by characterizing trajectory termination events. We first sought evidence for the direct trafficking of Ecad-GFP from the Golgi complex to the PM in HeLa cells. For epifluorescence analysis it was necessary to image the initial phase of transport with the focal plane raised above the level of the basal PM. The example in Figure 2 describes the exit from the Golgi complex of a spherical Ecad-GFP-positive PGC, and its subsequent transport to the cell periphery over a period of 40 s (Figure 2, C–E; Supplementary Movie 1). The PGC then remains stationary for $\sim$10 s before disappearing, with this observation probably representing the stationary phase that precedes fusion events, as described previously (Schmoranzer *et al.*, 2000; Toomre *et al.*, 2000).

Imaging at the basal surface of a HeLa cell revealed the arrival and subsequent fusion sites of five individual carriers, over a period of 120 s (Figure 2G; Supplementary Movie 2). The trajectories of two of these carriers can be traced directly back to the perinuclear region, suggesting that their origins lie in the Golgi complex. The behavior of each of these carriers is similar, with their rapid arrival at the plane of the basal PM, followed by a brief stationary phase (3–6 s), after which rapid dispersal and loss of fluorescence was observed. Analysis of the distribution of fluorescence associated with one of these putative fusion events reveals a characteristic initial central fluorescence peak and subsequent lateral redistribution of fluorescent

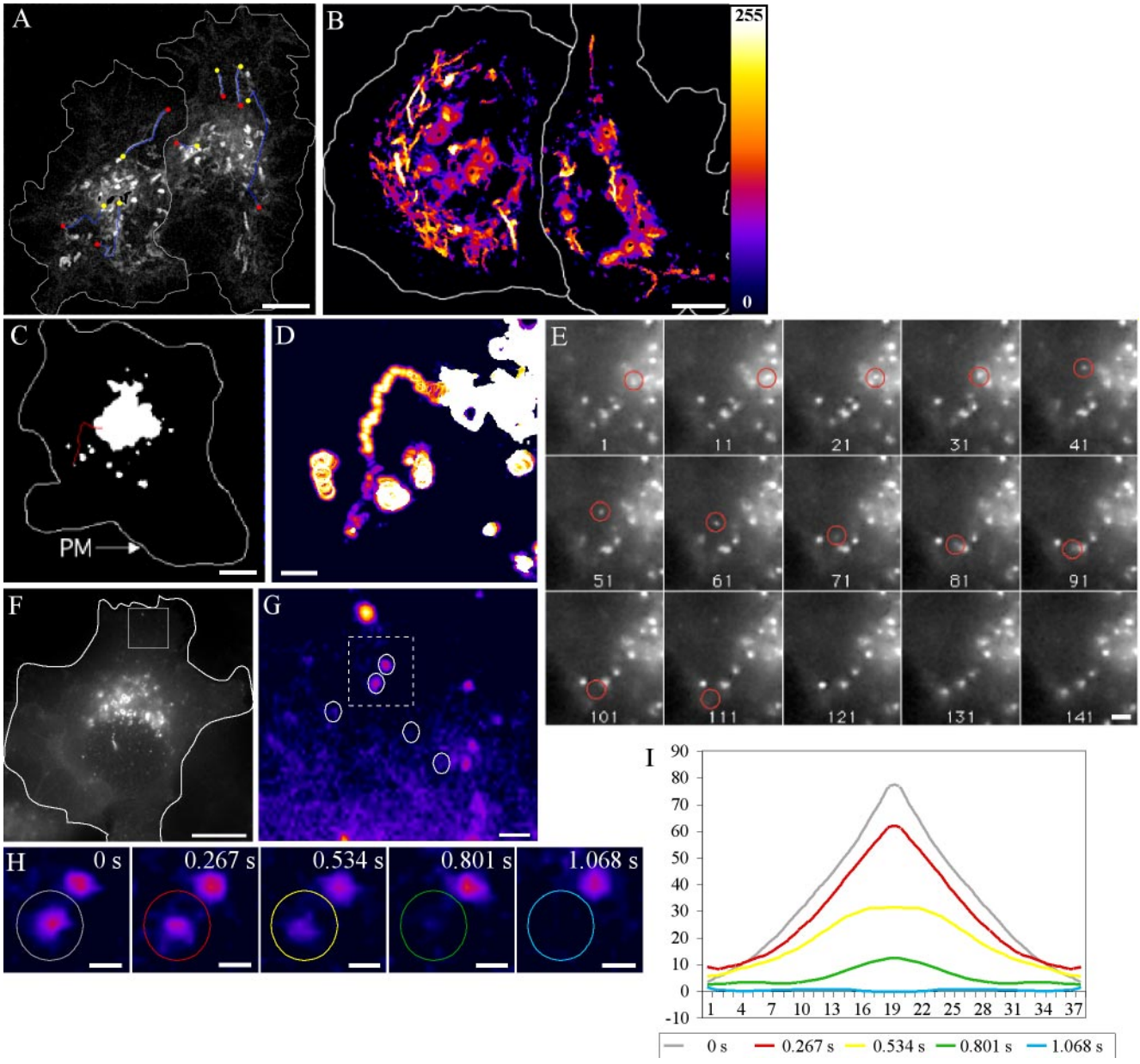

Figure 2. Ecad-GFP–positive PGC trajectories and direct Golgi-to-PM transport. Ecad-GFP was imaged in live HeLa cells to follow the trajectories of PGCs. A 60-s movie sequence (4 images/s) was recorded and then sequential images back-subtracted to produce a single image, showing the paths of seven Ecad-GFP–positive PGCs, with beginnings and ends of paths designated by yellow and red dots, respectively (A). A 90-s back-subtracted sequence, converted to an intensity-based color palette, highlights the concentration of curvilinear PGC tracks in the center of the cell (B). Imaging of a live HeLa cell at a focal plane level with the Golgi complex, shows the trajectory of a single spherical PGC (red trace) moving toward the cell periphery over a period of 40 s (C–E; Supplementary Movie 1). This is further enlarged in a back-subtracted image (D). Individual frames from this movie sequence (4 frames/s) show this 300-nm, spherical PGC (circled in red) as it exits the Golgi (frame 1) and finally disappears from the focal plane (after frame 111; E). To assess the fates of such PGCs in other live cells, imaging was performed at a focal plane level with the basal cell surface (F–H). Fusion events between Ecad-GFP-PGCs and the PM (F) are depicted in a region of interest (white box), converted to a pixel intensity-based color display palette (Supplementary Movie 2). Over 120 s, five fusion events were recorded, designated by white circles (G). Fully loaded PGCs arrived in the region, remained stationary, and then fused with the PM. In H, two stationary carriers (dashed box from G) are shown at 0.267-s intervals, fusing in succession. Analysis of the carrier fluorescence intensity distribution of the circled in H, is graphed I. The progressive flattening of the fluorescence distribution curve, indicates lateral dispersal of the PGC contents during fusion (Schmoranzer *et al.*, 2000; Toomre *et al.*, 2000). Scale bars, (A–C and F) 10 μm; (D, E, and G) 1 μm; (H) 250 nm.

cargo, commonly observed in surface delivery or fusion events (Figure 2, H and I). Such examples strongly support the proposal that Ecad-GFP–positive PGCs are capable of transport to and direct fusion with the PM. However, somewhat to our surprise, this was found to be a rare fate for Ecad-GFP–positive PGCs, occurring in as little as 5% of cases where a defined trajectory termination event was observed.

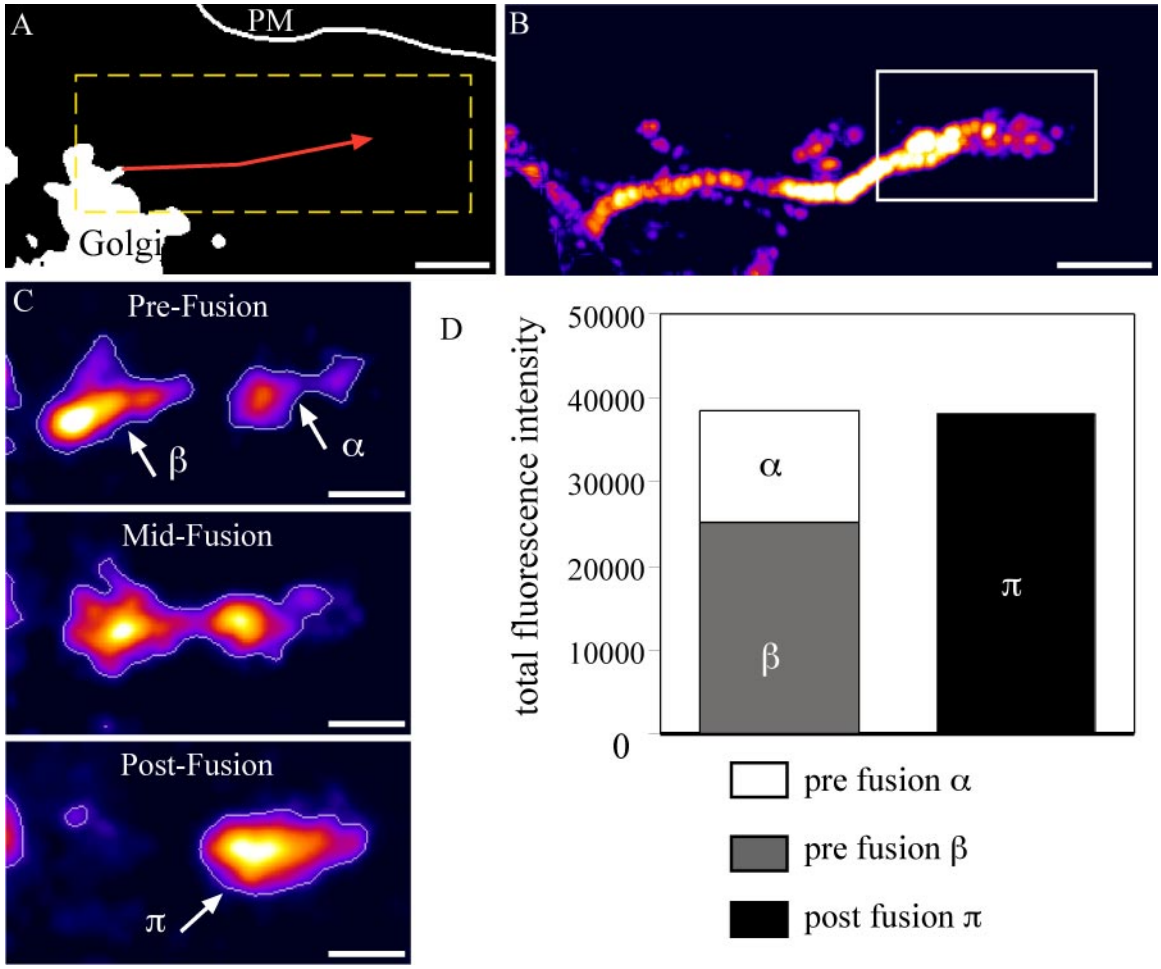

Figure 3. Ecad-GFP-PGCs fuse most frequently with intermediate compartments before PM delivery. Imaging in live HeLa cells shows the recorded track of an Ecad-GFP-PGC (red line; 56-s duration, 0.267 s/frame Supplementary Movie 3; A). The same trajectory is shown enlarged in a back-subtracted image (B) cropped from the dashed box in A. At the terminus of this trajectory (box from B) the PGC fuses with an intermediate, Ecad-GFP–positive structure, demonstrated by three sequential stages (C). Fluorescence intensities in the PGC and intermediate structure, objects β and α, respectively, in C, merge to give an equivalent total fluorescence in the final fused object, π in C, as graphed (D). Scale bars, (A and B) 2 μm; (C) 1 μm.

The most common fate recorded for Ecad-GFP–positive PGCs, after exit from the Golgi, is fusion with an intermediate structure before delivery to the PM (Figure 3; Supplementary Movie 3). In the example shown, after Golgi exit and curvilinear transport away from the perinuclear region, the tubulovesicular PGC approaches a relatively static, Ecad-GFP–positive membrane structure. These structures, which do not overlap with Golgi markers, are 1–3 μm in diameter and relatively static compared with PGCs, although they are capable of localized movement and some pleiomorphic dynamics. Figure 3C depicts images captured >0.81 s, at the instant before fusion, during fusion, and after fusion and fluorescence compaction, respectively. Fluorescence compaction measurements show that the total fluorescence in both the carrier and intermediate structure, is equal to the total fluorescence in the structure visible after fusion, providing evidence for fusion of the PGC with the intermediate structure. In live HeLa cells, most (>95%) of the Ecad-GFP exits the Golgi in PGCs, which move to and fuse with another more stable structure containing Ecad-GFP. This implies that rather than being transported directly to the PM, the route for most newly synthesized E-cadherin involves an initial trafficking step out of the Golgi complex to an intermediate post-Golgi compartment.

Post-Golgi Trafficking of E-cadherin to Rab11-positive Recycling Endosomes

We next sought to identify the intermediate compartment involved in Ecad-GFP exocytosis. Recent studies have shown that the delivery and polarized PM targeting of VSVG and LDLR can be disrupted after Golgi exit, by the expression of mutant Rab proteins associated with recycling endosomes (Chen *et al.*, 1998; Ang *et al.*, 2003; Folsch *et al.*, 2003). Rab11 is a known steady state marker of recycling endosomes (Ullrich *et al.*, 1996). An association of E-cadherin with Rab11 recycling endosomes was examined in HeLa cells fixed and GM130 labeled soon after cotransfection with E-cadherin-YFP (Ecad-YFP) and Rab11wt-GFP. Confocal imaging and spectral unmixing revealed that Ecad-YFP colocalized either with Rab11wt-GFP in punctate structures or with the Golgi complex marker GM130 labeling (Figure 4A). This localization remained consistent regardless of the level of Rab11wt-GFP expression. The concentration of Ecad-YFP in the Golgi complex at this time, but not at the PM, argues

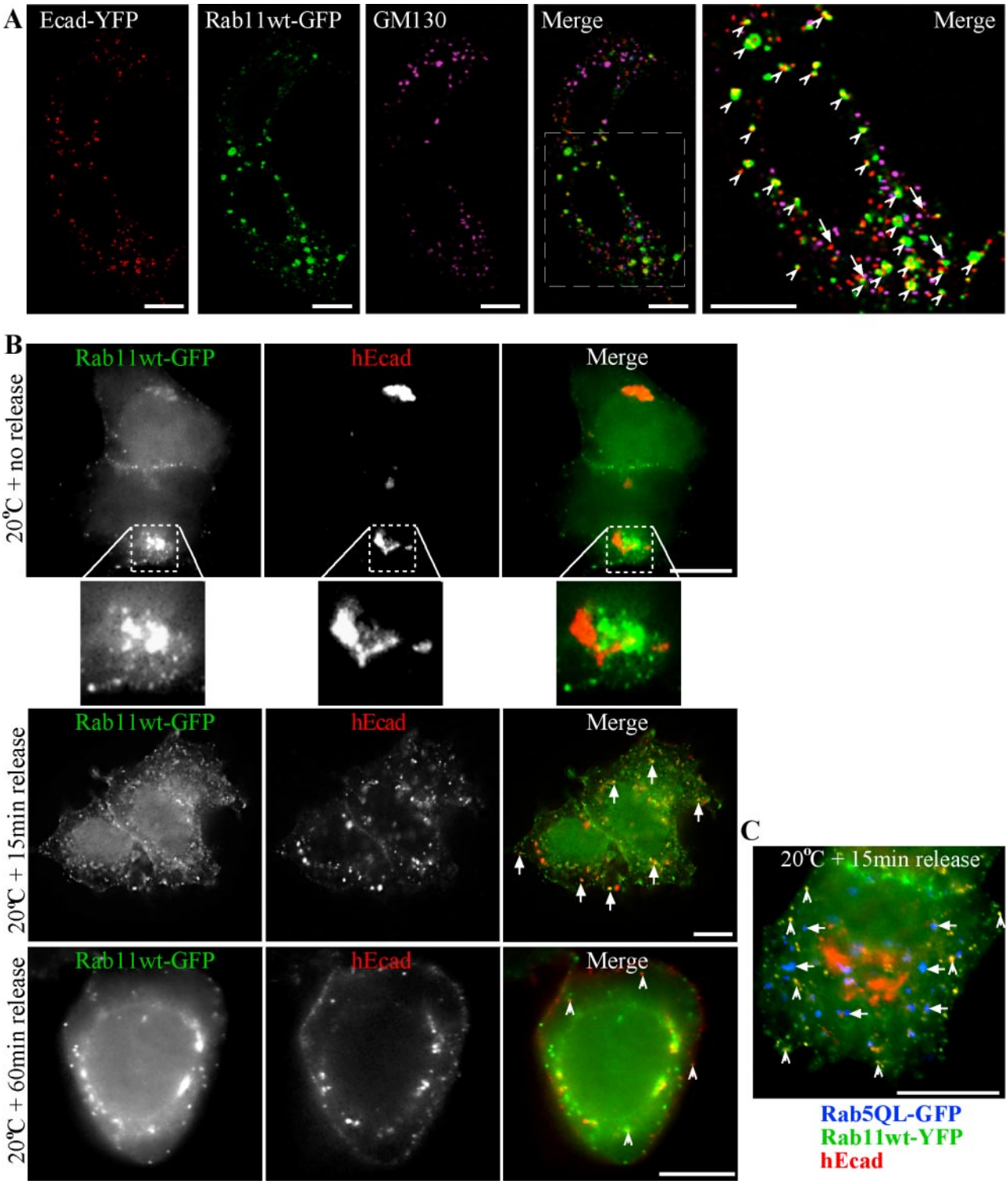

Figure 4. Biosynthetic E-cadherin colocalizes with Rab11wt-GFP in HeLa cells. HeLa cells cotransfected with Ecad-YFP and Rab11wt-GFP were fixed and labeled with an antibody to Golgi marker GM130 (A). Confocal microscopy and spectral unmixing show the individual patterns of each protein and the merged image. Ecad-YFP and Rab11wt-GFP colocalized in punctate structures (arrowheads) seen in the enlarged, merged image. Ecad-YFP also colocalized in some separate structures with GM130 (arrows). In B, HeLa cells coexpressing hEcad (red) and Rab11wt-GFP (green) were incubated at 20°C to block TGN exit and then fixed immediately (no release) or after 15- or 60-min release incubations at 37°C. An antibody used to label hEcad shows perinuclear Golgi accumulation, without PM labeling, and no colocalization with peripheral Rab11wt-GFP puncta, at 20°C. Enlargement of a typical perinuclear fluorescence pattern (dotted box) shows hEcad and Rab11wt-GFP closely adjacent, but not colocalizing. On release, hEcad then colocalizes in scattered punctate structures with Rab11wt-GFP (see solid arrows, 15 min, and hollow arrows, 60 min in merged images). hEcad labeling at the PM is evident 60 min after release. In HeLa cells expressing Rab11wt-YFP (green), hEcad (red), and Rab5QL-GFP (blue; C), hEcad colocalization with Rab11wt-YFP–positive punctae is clearly evident 15 min after 20°C block release (hollow arrows), although no significant colocalization is observed with Rab5QL-GFP–positive enlarged early endosomes (solid arrows). Scale bars, 10 μm.

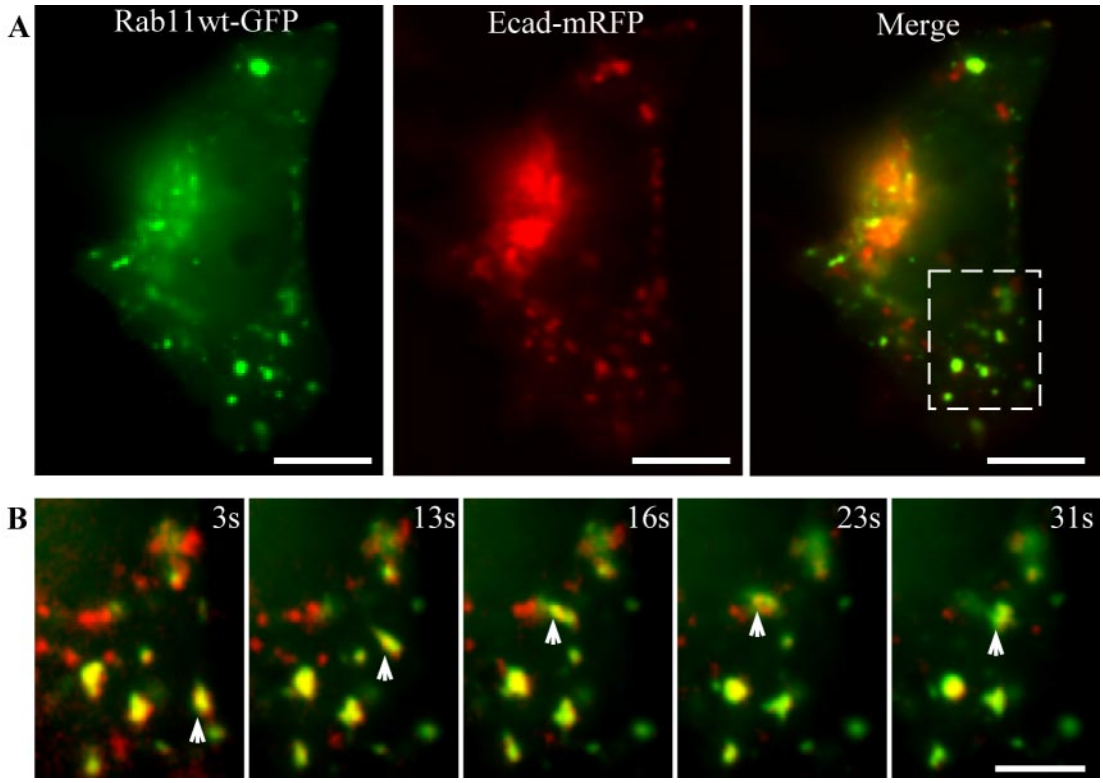

Figure 5. Colocalization of Ecad-mRFP with Rab11wt-GFP in live HeLa cells. HeLa cells, cotransfected with Rab11wt-GFP and Ecad-mRFP, were imaged live. A single image at the plane of the Golgi complex shows colocalization in some of the larger (1–3 μm), stationary structures (A). Ecad-mRFP is concentrated in the Golgi, in PGCs and in the larger structures colabeled with Rab11wt-GFP. Sequential images (cropped from dashed box in A) show colabeled intermediate compartments that move locally, whereas surrounding PGCs move on longer trajectories through this field (B). PGCs containing Rab11wt-GFP, Ecad-mRFP, or both, can be observed budding from and fusing with the intermediate compartments in the live movie sequence (Supplementary Movie 4). Scale bars, (A) 10 μm; (B) 5 μm.

that Ecad-YFP within the Rab11wt-GFP-positive structures is biosynthetic in nature and is en route to the PM, rather than being derived from an endocytic pathway. To further address this, a 20°C block was performed 2 h after transfection of HeLa cells with hEcad and Rab11wt-GFP (Figure 4B). After 5 h at 20°C, hEcad was concentrated in the Golgi complex, and was not present in Rab11wt-GFP–positive peripheral puncta. Perinuclear concentrations of Rab11wt-GFP and hEcad were closely adjacent, as expected, but did not significantly overlap. After release of the temperature block and resumption of exocytosis at 37°C, hEcad rapidly redistributed to peripheral punctate structures, many of which now colocalized with Rab11wt-GFP. After 60 min at 37°C, hEcad was still present in some internal Rab11wt-GFP–positive puncta, and was clearly present at the PM. Additionally, spectral unmixing and imaging of cells expressing Rab11wt-YFP, hEcad, and Rab5QL-GFP, demonstrated that 15 min after release of a 5 h 20°C block, hEcad rapidly colocalized with Rab11wt-YFP–positive punctae, but not Rab5QL-GFP–positive early endosomes, thereby ruling out endocytosis as a source of hEcad in recycling endosomes (Figure 4C). These results further indicate that Ecad moves from the TGN to Rab11-positive compartments and then to the PM during exocytosis.

Live imaging shortly after cotransfection of HeLa cells with both E-cadherin-mRFP (Ecad-mRFP) and Rab11wt-GFP further confirmed that the presence of E-cadherin in Rab11-positive structures resulted from exocytic, rather than endocytic transport, by demonstrating colocalization of these proteins in dynamic peripheral puncta ~1–3 μm in diameter (Figure 5; Supplementary Movie 4). These colabeled puncta are predominantly static, but are capable of local movement, fission, and fusion, and closely resemble the intermediate structures observed in single-color imaging of Ecad-GFP (Figures 1–3). In addition, small, highly dynamic, tubulovesicular carriers containing combinations of Ecad-mRFP and Rab11wt-GFP were also observed budding from and fusing with these larger puncta. These carriers were often targeted directly from one peripheral punctate structure to another, but did not bud from or fuse with the Golgi complex. These small carriers were also observed in HeLa cells singly expressing Rab11wt-GFP. As observed in fixed cells imaged at this time point, little or no surface delivery of Ecad-mRFP is observed, once again indicating that Rab11wt-GFP–positive compartments are traversed by E-cadherin when it is en route to the PM. These results demonstrated a Rab11-positive recycling endosome as an intermediate compartment for post-Golgi exocytosis of E-cadherin in HeLa cells. The presence of Rab11wt-GFP in smaller carriers with Ecad-mRFP in live cells, also suggests that Rab11 may have an active role in trafficking.

Overexpression of Rab11wt-GFP Selectively Impedes Cell Surface Delivery of E-cadherin, But Not of a Sorting Mutant

To assess a functional role for Rab11 in E-cadherin trafficking, HeLa cells were cotransfected with plasmids encoding either Rab11wt-GFP, Rab11SN-GFP (dominant negative) or

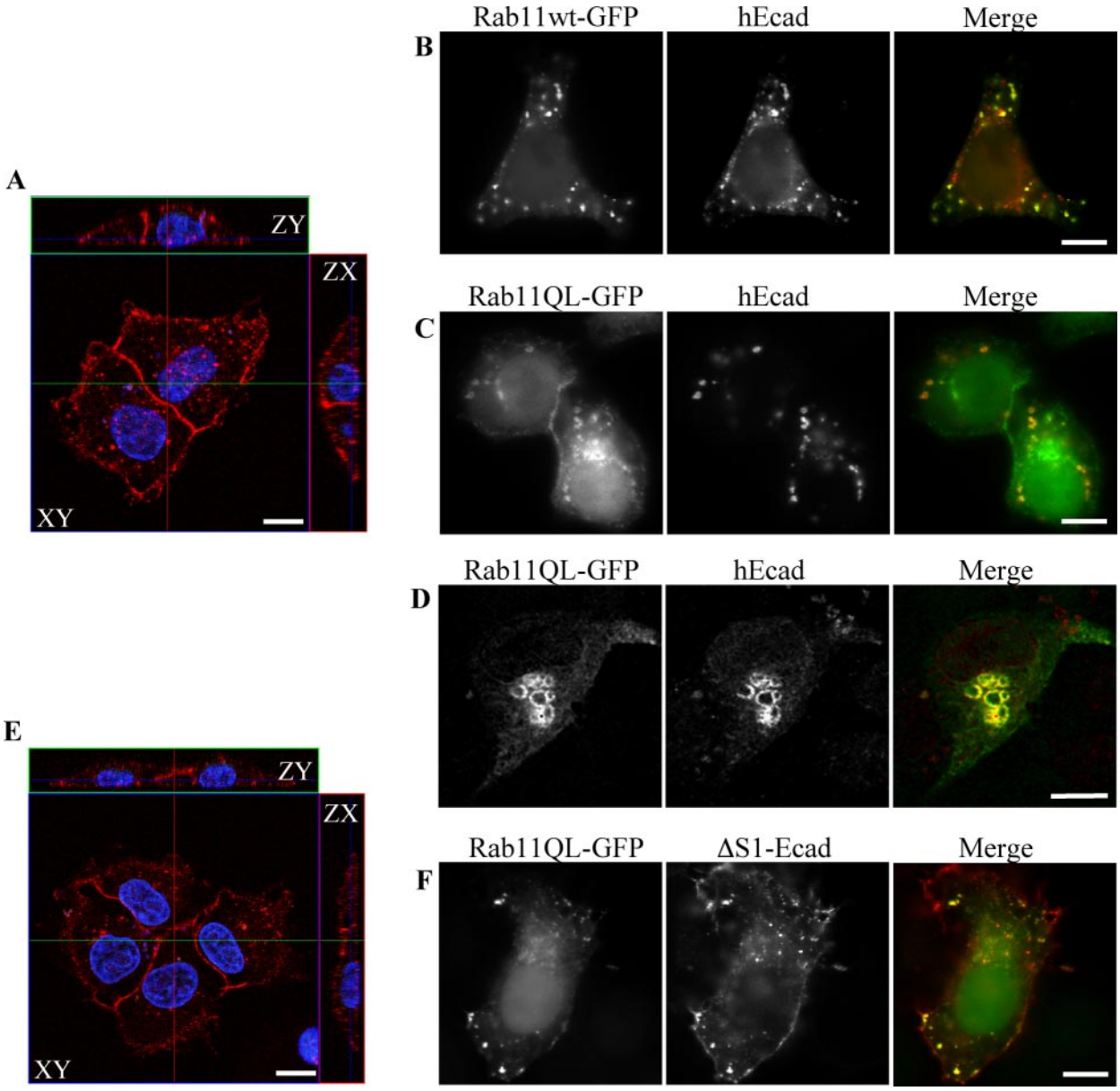

Figure 6. Localization and surface delivery of hEcad and ΔS1-Ecad in preconfluent HeLa and MDCK cells expressing Rab11 mutants. HeLa (A–C, E, and F) and MDCK (D) cells were fixed 24 h after transfection with combinations of either untagged hEcad or ΔS1-Ecad and either Rab11wt-GFP or Rab11QL-GFP. Cells were imaged by confocal microscopy as *ZY/ZX/XY* sections (A and E) or by epifluorescence (B–D and F). Immunolabeling of cells expressing either hEcad (A) or ΔS1-Ecad (E) alone, reveals efficient surface delivery of both cargos to the whole surface of HeLa cells. Coexpression of Rab11wt-GFP (B) or Rab11QL-GFP (C) greatly reduced hEcad surface delivery, so that no surface labeling was detectable. In these same cells, hEcad was concentrated in intracellular structures, many of which also contained either Rab11wt-GFP or Rab11QL-GFP. Similar results were observed in preconfluent MDCK cells expressing hEcad and Rab11QL-GFP, with hEcad surface delivery blocked, and strong intracellular accumulation in enlarged Rab11QL-GFP–positive compartments (D). In contrast to hEcad, ΔS1-Ecad was efficiently transported to the cell surface of HeLa cells in the presence of Rab11QL-GFP (F) and was colocalized in intracellular structures with Rab11QL-GFP. Scale bars, 10 μm.

Rab11QL-GFP (constitutively active), in conjunction with untagged, human E-cadherin (hEcad). Fixation and imaging 24 h after transfection revealed that relatively high-level expression of Rab11wt-GFP correlated with increased intracellular colocalization and reduced cell surface delivery of hEcad (Figure 6B), as compared with controls, which showed strong cell surface labeling resulting from efficient delivery of hEcad to the PM (Figure 6A). The reduction in PM labeling of hEcad was proportional to the level of Rab11wt-GFP expression. This block in transport was even more pronounced in HeLa cells coexpressing the Rab11QL-GFP mutant. In these cells, while some Rab11QL-GFP was itself present at the PM, hEcad was almost totally absent from the cell surface, instead being sequestered in Rab11QL-GFP–positive internal compartments (Figure 6C). Expression of the dominant negative Rab11SN-GFP mutant had a similar effect to the expression of Rab11wt-GFP, on the trafficking of hEcad (unpublished data). Preconfluent MDCK cells were also transfected to coexpress hEcad and Rab11QL-GFP (Figure 6D). hEcad also colocalized and ac-

cumulated in swollen Rab11QL-GFP–positive compartments in this cell type. These results again suggest that hEcad is trafficked to the PM through Rab11-positive recycling endosomes and that Rab11 has a direct role in the exocytic transport of E-cadherin. Furthermore, Rab11 functions in the post-Golgi trafficking of E-cadherin in both HeLa and nonpolarized MDCK cells.

Some nonpolarized cell lines have previously been shown to transport apical and basolateral membrane proteins independently in a manner analogous to differential trafficking in polarized cells (Yoshimori *et al.,* 1996; Rustom *et al.,* 2002). In polarized cells E-cadherin is sorted and trafficked to the basolateral membrane, but we have previously demonstrated that a mutant form of E-cadherin, (ΔS1-Ecad, missing a critical dileucine motif), is missorted and trafficked apically in MDCK cells (Miranda *et al.,* 2001). The effect of Rab11 mutants on the trafficking of both hEcad and ΔS1-Ecad was studied in HeLa cells. Hela cells were fixed and imaged 24 h after cotransfection with ΔS1-Ecad and either Rab11wt-GFP, Rab11QL-GFP, or Rab11SN-GFP. ΔS1-Ecad is also detectable in Rab11-positive compartments (Figure 6F). Interestingly, the expression of Rab11 and Rab11 mutants did not inhibit the trafficking of ΔS1-Ecad to the PM, compared with ΔS1-Ecad-only controls (Figure 6E). In cotransfected cells at a range of expression levels and for both the wild-type and GTP-bound Rab11 plasmids, ΔS1-Ecad was clearly present at the PM as well as in intracellular compartments. These results suggest that even in the absence of cell polarity, ΔS1-Ecad and hEcad are differentially trafficked, with Rab11 mutants disrupting only the latter.

Expression of Rab11 Mutants in Polarized MDCK Cells Disrupts the Localization of E-cadherin

Our findings in HeLa cells were next extended by examining the localization of E-cadherin in Rab11-transfected MDCK cells. Combinations of hEcad, ΔS1-Ecad, and Rab11 plasmids were cotransfected and expressed in confluent monolayers of MDCK cells. Rab11wt-GFP expressed in MDCK cells localized to structures equivalent to apical recycling endosomes (Casanova *et al.,* 1999; Wang *et al.,* 2001) and other dispersed perinuclear structures (see Supplementary Movies 7 and 8). Confocal imaging of fixed MDCK cells expressing hEcad or ΔS1-Ecad alone, demonstrated localization of hEcad at lateral surfaces (Figure 7A; Supplementary Movie 5), and of ΔS1-Ecad at the apical surface (Figure 7B; Movie 6). Coexpression of hEcad with either Rab11wt-GFP or Rab11QL-GFP, resulted in colocalization and some internal accumulation of hEcad (unpublished data). This was analogous to the results obtained in preconfluent MDCK cells (see Figure 6). However, coexpression of hEcad with Rab11SN-GFP, resulted in the aberrant localization of hEcad at the apical surface (Figure 7C; Supplementary Movie 7). Although this represents a clear dysregulation of hEcad basolateral targeting, ΔS1-Ecad localization at the apical surface was not effected by Rab11SN-GFP (Figure 7D; Supplementary Movie 8). Nevertheless, both hEcad and ΔS1-Ecad showed a moderate degree of colocalization with internal puncta labeled with Rab11SN-GFP. The expression of either Rab11SN-GFP or Rab11QL-GFP incidentally caused morphological transformation of polarized MDCK cells (Figure 7E; Supplementary Movie 9). Cells became less cuboidal, and more invasive, with large peripheral extensions protruding between adjacent cells. Thus, in polarized MDCK cells, appropriate localization of hEcad at the basolateral membrane involves a Rab11-positive recycling endosome. The selective disruption of hEcad localization, but not ΔS1-Ecad localization, caused by Rab11 mutants, suggests that Rab11 has a role in the sorting of E-cadherin, during exocytosis or recycling to the basolateral membrane, or possibly during both processes.

DISCUSSION

In this study, we set out to characterize post-Golgi trafficking routes taken by E-cadherin moving from the Golgi complex to the PM. This entailed detailed analysis of transport routes and carriers involved in post-Golgi transport of Ecad-GFP and targeting mutants of E-cadherin in live and fixed cells. The trajectories and destinations utilized by these carriers were documented showing that Ecad-GFP exits the Golgi complex in large, dynamic, pleiomorphic carriers. The majority of E-cadherin does not travel directly to the PM from the TGN, but is routed instead via a Rab11-positive intermediate compartment in nonpolarized HeLa cells, and furthermore, that Rab11 and Rab11 mutants can disrupt the basolateral localization of E-cadherin in polarized MDCK cells.

The carriers observed in our live imaging analysis of E-cadherin transport show strikingly similar characteristics to those well documented in the literature, resulting from the observation of VSVG-GFP transport from the TGN to the PM (Hirschberg *et al.,* 1998; Hirschberg and Lippincott-Schwartz, 1999; Toomre *et al.,* 1999, 2000; Polishchuk *et al.,* 2003). In our hands, comparative transport analysis of Ecad-GFP and VSVG-GFP revealed that these cargoes utilize carriers whose morphology and kinetics were indistinguishable at the light microscopic level. How these dynamic, pleiomorphic carriers relate to the accepted models of adaptor-based sorting and trafficking, remains unclear (Bonifacino and Lippincott-Schwartz, 2003). Live imaging followed by correlative electron microscopy has shown that VSVG-containing carriers in nonpolarized cells are uncoated and may represent a bulk flow process (Polishchuk *et al.,* 2003). Uncoated tubules are regularly seen extending from the Golgi complex in tomographic images (Marsh *et al.,* 2001). However, in recent live imaging studies, pleiomorphic, tubulovesicular carriers have also been shown to be coated with fluorescently tagged clathrin and adaptor proteins, during and after exit from the Golgi complex (Huang *et al.,* 2001; Puertollano *et al.,* 2003; Waguri *et al.,* 2003).

The mobility and kinetics of PGCs carrying Ecad-GFP are also comparable to those shown for VSVG-GFP. Behaviors of the PGCs, such as their rates of movement (~3 μm/s), their curvilinear paths and the dynamics of the PGCs themselves (bifurcation, fusion, pinching off), have all been previously described (Hirschberg *et al.,* 1998; Hirschberg and Lippincott-Schwartz, 1999; Toomre *et al.,* 1999; Polishchuk *et al.,* 2003). Our findings thus newly document such facets of post-Golgi transport for a cell surface adhesion protein, E-cadherin. Based on these previous observations of VSVG-GFP moving directly from the TGN to the PM in live cells, our finding that Ecad-GFP is mainly trafficked to a post-Golgi intermediate compartment was unexpected. Fusion of Ecad-GFP PGCs with the PM was documented as a possible but infrequent event in nonpolarized cells. Whether this represents a true divergence in trafficking pathways for E-cadherin versus VSVG, a difference between cell types, or a difference in imaging analysis, remains to be seen.

Colocalization in fixed and live cells showed that E-cadherin exiting the Golgi complex is trafficked to relatively static intermediate structures, ~1–3-μm diameter, that were identified as Rab11-positive recycling endosomes. The morphology of the recycling endosome demarcated by Rab11 varies significantly between cell types (Urbe *et al.,* 1993;

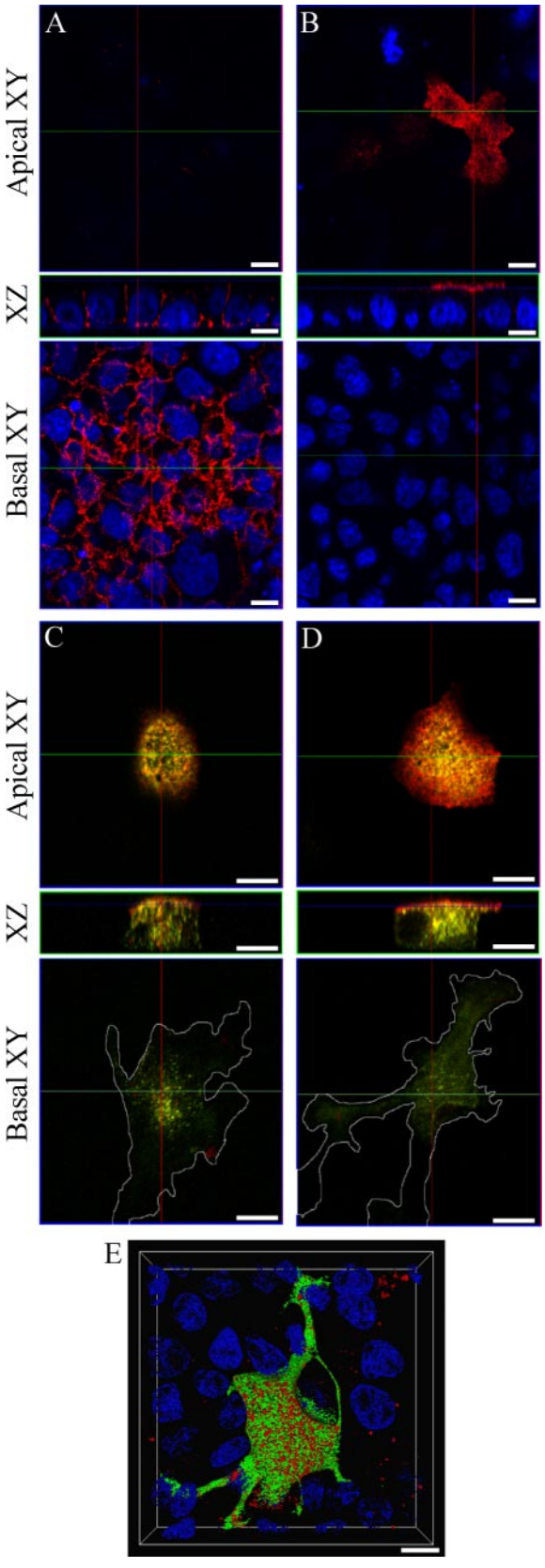

Figure 7. Rab11 mutants mistarget hEcad and transform polarized MDCK cells. Confluent monolayers of MDCK cells were fixed and labeled, and confocal imaging was performed to generate *XZ* and *XY* sections. Single expression of hEcad (A) or ΔS1-Ecad (B) shows their basolateral or apical distribution, respectively (red labeling), relative to nuclear staining (DAPI, blue). In cells coexpressing Rab11SN-GFP (green), hEcad (red) is dramatically shifted to the apical surface (C). Coexpression of Rab11SN-GFP (green) does not alter the apical delivery of ΔS1-Ecad (red; D). The expression of Rab11SN-GFP notably transforms the cells initially causing enhanced spreading and invasive protrusion at the basal cell surface, as seen in basal *XY* sections (C and D). This phenotypic change was even more striking after expression of Rab11QL-GFP as seen in a 3D reconstruction of cells cotransfected with Rab11QL-GFP (green) and hEcad (red; E). 3D rendered animations of confocal sections pertaining to each panel are available in the supplementary material (Supplementary Movies 5–9) Scale bars, 10 μm.

Goldenring *et al.*, 1996; Ullrich *et al.*, 1996; Hoekstra *et al.*, 2004). It is composed of peripheral puncta, and a perinuclear concentration that is intimately associated with the Golgi complex and the microtubule organizing center (Ullrich *et al.*, 1996). Overexpression of Rab11 mutants in this and other studies causes the redistribution of Rab11 and cargo to various points between the TGN and cell surface, suggesting a dynamic role for Rab11 in trafficking to and from the recycling endosome (Chen *et al.*, 1998). This is also consistent with our novel live imaging of Rab11, shown herein (Supplementary Movie 4), where we observed active budding and fusion of small Rab11 carriers with larger Rab11-positive intermediate structures.

In fixed HeLa cells we show that Ecad-GFP reaches the Rab11 compartment rapidly after release from a 20°C block and that it does not colocalize with early endosomes under the same conditions. This information, in conjunction with live imaging data, strongly suggests that Ecad-GFP fuses with the Rab11 recycling endosome during exocytosis. There is precedent for this recycling endosome as an intermediate compartment in the exocytic traffic of other biosynthetic cargo destined for the PM. For instance, transferrin receptor has been shown to be delivered to endosomal compartments before surface delivery (Futter *et al.*, 1995). Furthermore, Rab11 has previously been implicated in the regulation of both constitutive and regulated post-Golgi trafficking through its association with both constitutive and regulated secretory granules and through its regulation of the constitutive cargo, VSVG (Urbe *et al.*, 1993; Chen *et al.*, 1998). Chen *et al.* (1998) demonstrated that expression of Rab11 mutants could cause the partial (~50%) blocking of VSVG surface delivery, thereby suggesting that VSVG might utilize both Rab11-sensitive and Rab11-insensitive pathways. Ecad-GFP was similarly accumulated in recycling endosomes by expression of Rab11 mutants. Surface E-cadherin is known to be endocytosed and in some cases recycled back to the PM, thus although we have focused here on exocytosis of Ecad-GFP, it is also possible that surface Ecad-GFP recycles back through the recycling endosome under some circumstances.

In polarized MDCK cells the apical recycling endosome (ARE) is known to be Rab11-positive, representing a subdomain of the subapical compartment, a major site of sorting for endocytic and transcytotic transport (Hoekstra *et al.*, 2004). Our imaging of Rab11 in polarized MDCK cells is consistent with its reported localization in the ARE (Casanova *et al.*, 1999; Rahner *et al.*, 2000). Our results now show that E-cadherin passes through a Rab11-positive ARE in MDCK cells and that this compartment appears to play a key role in the exocytosis and/or recycling of E-cadherin. Rab11 has previously been implicated in polarized sorting of IgA receptor and transferrin (Leung *et al.*, 2000; Wang *et al.*, 2001; Hales *et al.*, 2002).

E-cadherin and its sorting mutant, ΔS1-Ecad, are differentially trafficked in polarized MDCK cells (Miranda *et al.*, 2001). When both were expressed in HeLa cells, we found that although both proteins showed some colocalization with Rab11, Rab11 mutants effected trafficking of wild-type hEcad, but not of ΔS1-Ecad. This implies that a sorting step occurs within or after Rab11-positive compartments, which distinguishes hEcad and ΔS1-Ecad based on the presence or absence of the dileucine sorting motif. This is likely to be an adaptor-binding event, although the specific adaptor involved in E-cadherin dileucine-mediated sorting is not yet known. The differential effects of Rab11 on hEcad and ΔS1-Ecad trafficking in nonpolarized HeLa cells provides new evidence, together with previous data (Miranda *et al.*, 2001), that the epithelial specific μ1b adaptor is not involved.

Another post-Golgi membrane-associated small GTPase, Rab8, has been shown to have a regulatory role in the post-Golgi trafficking of μ1B-dependent, basolaterally targeted cargoes, including LDLR, VSVG, and transferrin receptor (Ang *et al.*, 2003), thereby defining an additional and alternative pathway for basolateral surface delivery. The differential localization of Rab11a and Rab11b in MDCK cells (Lapierre *et al.*, 2003) further suggests morphological and functional subdivision of recycling compartments (Hoekstra *et al.*, 2004) possibly for different sorting events. Finally, the majority of live imaging studies (Toomre *et al.*, 1999; Lippincott-Schwartz *et al.*, 2000; Schmoranzer *et al.*, 2000; Toomre *et al.*, 2000), including this one, support the existence of a direct delivery pathway from the Golgi complex to the PM that bypasses the recycling endosome. Thus our studies begin to elucidate which one of several possible pathways E-cadherin uses to reach the cell surface.

In summary, we propose a model whereby the majority of E-cadherin transport to the PM occurs via Rab11-positive recycling endosomes, rather than moving directly from the Golgi complex to the PM. The recycling endosome thus becomes a crucial compartment for regulating exocytic delivery of E-cadherin to the cell surface, and thereby for establishing and modulating cellular adhesion in epithelia. This is further demonstrated by our finding in epithelial cells that E-cadherin mistargeting and lateral cell surface depletion, due to Rab11 mutant overexpression, results in a morphological transformation of cells, reminiscent of the dysmorphology caused by expression of ΔS1-Ecad (Miranda *et al.*, 2001). Rab11 in the subapical compartment of MDCK cells is at a site of intersection of both endocytic and exocytic traffic (Hoekstra *et al.*, 2004). The location of Rab11 coincides closely with the location of recycling E-cadherin internalized from the basolateral membrane in polarized MDCK cells (Le *et al.*, 1999, 2002). Thus Rab11 also has the potential, yet to be tested, to further modulate cadherin-based adhesion via the endocytosis and recycling of E-cadherin (Le *et al.*, 1999).

ACKNOWLEDGMENTS

We thank colleagues and members of the Stow laboratory for discussions and helpful comments. We thank colleagues where acknowledged for kindly providing cDNAs. This work was supported by a University of Queensland Postgraduate Scholarship (J.G.L.) and a fellowship and grants from the National Health and Medical Research Council (J.L.S.).

REFERENCES

Ang, A. L., Folsch, H., Koivisto, U. M., Pypaert, M., and Mellman, I. (2003). The Rab8 GTPase selectively regulates AP-1B-dependent basolateral transport in polarized Madin-Darby canine kidney cells. J. Cell Biol. *163*, 339–350.

Band, A. M., Ali, H., Vartiainen, M. K., Welti, S., Lappalainen, P., Olkkonen, V. M., and Kuismanen, E. (2002). Endogenous plasma membrane t-SNARE syntaxin 4 is present in rab11 positive endosomal membranes and associates with cortical actin cytoskeleton. FEBS Lett. *531*, 513–519.

Bonifacino, J. S., and Lippincott-Schwartz, J. (2003). Coat proteins: shaping membrane transport. Nat. Rev. Mol. Cell. Biol. *4*, 409–414.

Bryant, D. M., and Stow, J. L. (2004). The ins and outs of E-cadherin trafficking. Trends Cell Biol. *14*, 427–434.

Bryant, D. M., Wylie, F. G., and Stow, J. L. (2005). Regulation of endocytosis, nuclear translocation, and signaling of fibroblast growth factor receptor 1 by e-cadherin. Mol. Biol. Cell *16*, 14–23.

Calhoun, B. C., and Goldenring, J. R. (1996). Rab proteins in gastric parietal cells: evidence for the membrane recycling hypothesis. Yale J. Biol. Med. *69*, 1–8.

Casanova, J. E., Wang, X., Kumar, R., Bhartur, S. G., Navarre, J., Woodrum, J. E., Altschuler, Y., Ray, G. S., and Goldenring, J. R. (1999). Association of Rab25 and Rab11a with the apical recycling system of polarized Madin-Darby canine kidney cells. Mol. Biol. Cell *10*, 47–61.

Chen, W., Feng, Y., Chen, D., and Wandinger-Ness, A. (1998). Rab11 is required for trans-golgi network-to-plasma membrane transport and a preferential target for GDP dissociation inhibitor. Mol. Biol. Cell *9*, 3241–3257.

Chen, X., Kojima, S., Borisy, G. G., and Green, K. J. (2003). p120 catenin associates with kinesin and facilitates the transport of cadherin-catenin complexes to intercellular junctions. J. Cell Biol. *163*, 547–557.

Chen, Y. T., Stewart, D. B., and Nelson, W. J. (1999). Coupling assembly of the E-cadherin/beta-catenin complex to efficient endoplasmic reticulum exit and basal-lateral membrane targeting of E-cadherin in polarized MDCK cells. J. Cell Biol. *144*, 687–699.

Cohen, D., Musch, A., and Rodriguez-Boulan, E. (2001). Selective control of basolateral membrane protein polarity by cdc42. Traffic *2*, 556–564.

Folsch, H., Pypaert, M., Maday, S., Pelletier, L., and Mellman, I. (2003). The AP-1A and AP-1B clathrin adaptor complexes define biochemically and functionally distinct membrane domains. J. Cell Biol. *163*, 351–362.

Futter, C. E., Connolly, C. N., Cutler, D. F., and Hopkins, C. R. (1995). Newly synthesized transferrin receptors can be detected in the endosome before they appear on the cell surface. J. Biol. Chem. *270*, 10999–11003.

Goldenring, J. R., Smith, J., Vaughan, H. D., Cameron, P., Hawkins, W., and Navarre, J. (1996). Rab11 is an apically located small GTP-binding protein in epithelial tissues. Am. J. Physiol. *270*, G515–G525.

Grindstaff, K. K., Yeaman, C., Anandasabapathy, N., Hsu, S. C., Rodriguez-Boulan, E., Scheller, R. H., and Nelson, W. J. (1998). Sec6/8 complex is recruited to cell-cell contacts and specifies transport vesicle delivery to the basal-lateral membrane in epithelial cells. Cell *93*, 731–740.

Gumbiner, B. M. (1996). Cell adhesion: the molecular basis of tissue architecture and morphogenesis. Cell *84*, 345–357.

Hales, C. M., Vaerman, J. P., and Goldenring, J. R. (2002). Rab11 family interacting protein 2 associates with Myosin Vb and regulates plasma membrane recycling. J. Biol. Chem. *277*, 50415–50421.

Hazan, R. B., Qiao, R., Keren, R., Badano, I., and Suyama, K. (2004). Cadherin switch in tumor progression. Ann. NY Acad. Sci. *1014*, 155–163.

Hirschberg, K., and Lippincott-Schwartz, J. (1999). Secretory pathway kinetics and in vivo analysis of protein traffic from the Golgi complex to the cell surface. FASEB J. *13*, S251–S256.

Hirschberg, K., Miller, C. M., Ellenberg, J., Presley, J. F., Siggia, E. D., Phair, R. D., and Lippincott-Schwartz, J. (1998). Kinetic analysis of secretory protein traffic and characterization of golgi to plasma membrane transport intermediates in living cells. J. Cell Biol. *143*, 1485–1503.

Hoekstra, D., Tyteca, D., and van IJzendoorn, S. C. (2004). The subapical compartment: a traffic center in membrane polarity development. J. Cell Sci. *117*, 2183–2192.

Huang, F., Nesterov, A., Carter, R. E., and Sorkin, A. (2001). Trafficking of yellow-fluorescent-protein-tagged mu1 subunit of clathrin adaptor AP-1 complex in living cells. Traffic *2*, 345–357.

Inoue, M., Chang, L., Hwang, J., Chiang, S. H., and Saltiel, A. R. (2003). The exocyst complex is required for targeting of Glut4 to the plasma membrane by insulin. Nature *422*, 629–633.

Kreitzer, G., Schmoranzer, J., Low, S. H., Li, X., Gan, Y., Weimbs, T., Simon, S. M., and Rodriguez-Boulan, E. (2003). Three-dimensional analysis of post-Golgi carrier exocytosis in epithelial cells. Nat. Cell Biol *5*, 126–136.

Kroschewski, R., Hall, A., and Mellman, I. (1999). Cdc42 controls secretory and endocytic transport to the basolateral plasma membrane of MDCK cells. Nat. Cell Biol. *1*, 8–13.

Lapierre, L. A., Dorn, M. C., Zimmerman, C. F., Navarre, J., Burnette, J. O., and Goldenring, J. R. (2003). Rab11b resides in a vesicular compartment distinct from Rab11a in parietal cells and other epithelial cells. Exp. Cell Res. *290*, 322–331.

Le, T. L., Joseph, S. R., Yap, A. S., and Stow, J. L. (2002). Protein kinase C regulates endocytosis and recycling of E-cadherin. Am. J. Physiol. Cell. Physiol. *283*, C489–C499.

Le, T. L., Yap, A.S., and Stow, J. L. (1999). Recycling of E-cadherin: a potential mechanism for regulating cadherin dynamics. J. Cell Biol. *146*, 219–232.

Leung, S. M., Ruiz, W. G., and Apodaca, G. (2000). Sorting of membrane and fluid at the apical pole of polarized Madin-Darby canine kidney cells. Mol. Biol. Cell *11*, 2131–2150.

Lippincott-Schwartz, J., Roberts, T. H., and Hirschberg, K. (2000). Secretory protein trafficking and organelle dynamics in living cells. Annu. Rev. Cell. Dev. Biol. *16*, 557–589.

Lipschutz, J. H., Guo, W., O'Brien, L. E., Nguyen, Y. H., Novick, P., and Mostov, K. E. (2000). Exocyst is involved in cystogenesis and tubulogenesis and acts by modulating synthesis and delivery of basolateral plasma membrane and secretory proteins. Mol. Biol. Cell *11*, 4259–4275.

Marsh, B. J., Mastronarde, D. N., Buttle, K. F., Howell, K. E., and McIntosh, J. R. (2001). Organellar relationships in the Golgi region of the pancreatic beta cell line, HIT-T15, visualized by high resolution electron tomography. Proc. Natl. Acad. Sci. USA *98*, 2399–2406.

Miranda, K. C., Joseph, S. R., Yap, A. S., Teasdale, R. D., and Stow, J. L. (2003). Contextual binding of p120ctn to E-cadherin at the basolateral plasma membrane in polarized epithelia. J. Biol. Chem. *278*, 43480–43488.

Miranda, K. C., Khromykh, T., Christy, P., Le, T. L., Gottardi, C. J., Yap, A. S., Stow, J. L., and Teasdale, R. D. (2001). A dileucine motif targets E-cadherin to the basolateral cell surface in Madin-Darby canine kidney and LLC-PK1 epithelial cells. J. Biol. Chem. *276*, 22565–22572.

Moskalenko, S., Henry, D. O., Rosse, C., Mirey, G., Camonis, J. H., and White, M. A. (2002). The exocyst is a Ral effector complex. Nat. Cell Biol *4*, 66–72.

Musch, A., Cohen, D., Kreitzer, G., and Rodriguez-Boulan, E. (2001). cdc42 regulates the exit of apical and basolateral proteins from the trans-Golgi network. EMBO J. *20*, 2171–2179.

Polishchuk, E. V., Di Pentima, A., Luini, A., and Polishchuk, R. S. (2003). Mechanism of constitutive export from the golgi: bulk flow via the formation, protrusion, and en bloc cleavage of large trans-golgi network tubular domains. Mol. Biol. Cell *14*, 4470–4485.

Polishchuk, R. S., Polishchuk, E. V., Marra, P., Alberti, S., Buccione, R., Luini, A., and Mironov, A. A. (2000). Correlative light-electron microscopy reveals the tubular-saccular ultrastructure of carriers operating between Golgi apparatus and plasma membrane. J. Cell Biol. *148*, 45–58.

Puertollano, R., van der Wel, N. N., Greene, L. E., Eisenberg, E., Peters, P. J., and Bonifacino, J. S. (2003). Morphology and dynamics of clathrin/GGA1-coated carriers budding from the trans-Golgi network. Mol. Biol. Cell *14*, 1545–1557.

Rahner, C., Stieger, B., and Landmann, L. (2000). Apical endocytosis in rat hepatocytes in situ involves clathrin, traverses a subapical compartment, and leads to lysosomes. Gastroenterology *119*, 1692–1707.

Ren, M., Xu, G., Zeng, J., De Lemos-Chiarandini, C., Adesnik, M., and Sabatini, D. D. (1998). Hydrolysis of GTP on rab11 is required for the direct delivery of transferrin from the pericentriolar recycling compartment to the cell surface but not from sorting endosomes. Proc. Natl. Acad. Sci. USA *95*, 6187–6192.

Rustom, A., Bajohrs, M., Kaether, C., Keller, P., Toomre, D., Corbeil, D., and Gerdes, H. H. (2002). Selective delivery of secretory cargo in Golgi-derived carriers of nonepithelial cells. Traffic *3*, 279–288.

Schmoranzer, J., Goulian, M., Axelrod, D., and Simon, S. M. (2000). Imaging constitutive exocytosis with total internal reflection fluorescence microscopy. J. Cell Biol. *149*, 23–32.

Sheehan, D., Ray, G. S., Calhoun, B. C., and Goldenring, J. R. (1996). A somatodendritic distribution of Rab11 in rabbit brain neurons. Neuroreport *7*, 1297–1300.

Takeichi, M. (1991). Cadherin cell adhesion receptors as a morphogenetic regulator. Science *251*, 1451–1455.

Takeichi, M. (1995). Morphogenetic roles of classic cadherins. Curr. Opin. Cell Biol. *7*, 619–627.

Toomre, D., Keller, P., White, J., Olivo, J. C., and Simons, K. (1999). Dual-color visualization of trans-Golgi network to plasma membrane traffic along microtubules in living cells. J. Cell Sci. *112*, 21–33.

Toomre, D., Steyer, J. A., Keller, P., Almers, W., and Simons, K. (2000). Fusion of constitutive membrane traffic with the cell surface observed by evanescent wave microscopy. J. Cell Biol. *149*, 33–40.

Ullrich, O., Reinsch, S., Urbe, S., Zerial, M., and Parton, R. G. (1996). Rab11 regulates recycling through the pericentriolar recycling endosome. J. Cell Biol. *135*, 913–924.

Urbe, S., Huber, L. A., Zerial, M., Tooze, S. A., and Parton, R. G. (1993). Rab11, a small GTPase associated with both constitutive and regulated secretory pathways in PC12 cells. FEBS Lett. *334*, 175–182.

Waguri, S., Dewitte, F., Le Borgne, R., Rouille, Y., Uchiyama, Y., Dubremetz, J. F., and Hoflack, B. (2003). Visualization of TGN to endosome trafficking through fluorescently labeled MPR and AP-1 in living cells. Mol. Biol. Cell *14*, 142–155.

Wang, E., Pennington, J. G., Goldenring, J. R., Hunziker, W., and Dunn, K. W. (2001). Brefeldin A rapidly disrupts plasma membrane polarity by blocking polar sorting in common endosomes of MDCK cells. J. Cell Sci. *114*, 3309–3321.

Yap, A. S., Brieher, W. M., and Gumbiner, B. M. (1997). Molecular and functional analysis of cadherin-based adherens junctions. Annu. Rev. Cell. Dev. Biol. *13*, 119–146.

Yeaman, C., Grindstaff, K. K., Wright, J. R., and Nelson, W. J. (2001). Sec6/8 complexes on trans-Golgi network and plasma membrane regulate late stages of exocytosis in mammalian cells. J. Cell Biol. *155*, 593–604.

Yoshimori, T., Keller, P., Roth, M. G., and Simons, K. (1996). Different biosynthetic transport routes to the plasma membrane in BHK and chinese hamster ovary cells. J. Cell Biol. *133*, 247–256.